

Lawrence Berkeley National Laboratory

LBL Publications

Title

Current loss analysis in photoelectrochemical devices

Permalink

<https://escholarship.org/uc/item/4cw969nv>

Journal

APL Materials, 8(3)

ISSN

2166-532X

Authors

Kistler, Tobias A

Agbo, Peter

Publication Date

2020-03-01

DOI



10.1063/1.5142561

Peer reviewed

Current loss analysis in photoelectrochemical devices

Cite as: APL Mater. **8**, 031107 (2020); <https://doi.org/10.1063/1.5142561>

Submitted: 14 December 2019 . Accepted: 18 February 2020 . Published Online: 04 March 2020

 Tobias A. Kistler, and  Peter Agbo

COLLECTIONS

Paper published as part of the special topic on [Solar to FuelSTF2020](#)



View Online



Export Citation



CrossMark

ARTICLES YOU MAY BE INTERESTED IN

[Evaluating carbon dots as electron mediators in photochemical and photocatalytic processes of NiFe₂O₄](#)

APL Materials **8**, 031105 (2020); <https://doi.org/10.1063/1.5134432>

[Spray-processed nanoporous BiVO₄ photoanodes with high charge separation efficiency for oxygen evolution](#)

APL Materials **8**, 031112 (2020); <https://doi.org/10.1063/1.5144107>

[On factors limiting the performance of photoelectrochemical CO₂ reduction](#)

The Journal of Chemical Physics **152**, 100901 (2020); <https://doi.org/10.1063/1.5141390>

Hall Effect Measurement Handbook

A comprehensive resource for researchers

Explore theory, methods, sources of errors, and ways to minimize the effects of errors



Current loss analysis in photoelectrochemical devices

Cite as: APL Mater. 8, 031107 (2020); doi: 10.1063/1.5142561
Submitted: 14 December 2019 • Accepted: 18 February 2020 •
Published Online: 4 March 2020



View Online



Export Citation



CrossMark

Tobias A. Kistler^{1,2,3}  and Peter Agbo^{1,2,a)} 

AFFILIATIONS

¹Chemical Sciences Division, Lawrence Berkeley National Laboratory, Berkeley, California 94720, USA

²Joint Center for Artificial Photosynthesis, Lawrence Berkeley National Laboratory, Berkeley, California 94720, USA

³Walter Schottky Institute and Physics Department, Technische Universität München, Garching 85748, Germany

Note: This paper is part of the Special Issue on Solar to Fuel.

^{a)}Author to whom correspondence should be addressed: pagbo@lbl.gov

ABSTRACT

Ongoing efforts to stabilize the operation of photoelectrochemical (PEC) devices remain critical for achieving economically viable solar fuel production, as devices with lifetimes on the order of 10 to 30 years are projected requirements for utility-scale, PEC device implementation. However, insight into the causes of device degradation and activity losses is generally provided by monitoring the device current, a quantity which masks the relative contributions of photovoltaic component degradation and electrocatalyst activity drops to overall performance losses. In this study, an approach for deconvoluting the various contributors to PEC device losses is described. In particular, the causes for observed fluctuations in device performance are determined through the collection of real-time, current-voltage data, paired with an analytical method that enables the decomposition of drops in device current into its constituent photovoltaic- and catalyst-driven performance losses. We test the validity of this approach by applying it to the data collected for a PEC hydrogen evolution test-bed.

© 2020 Author(s). All article content, except where otherwise noted, is licensed under a Creative Commons Attribution (CC BY) license (<http://creativecommons.org/licenses/by/4.0/>). <https://doi.org/10.1063/1.5142561>

Significant progress has been made in the development of solar fuel devices, which store the energy of Earth's incident solar flux in molecular bonds, since the initial report of the Honda-Fujishima effect on nano-particulate titanium dioxide nearly 50 years ago.^{1,2} Since then, particular focus has been given to increase the solar-to-fuel conversion efficiency of these devices, with current efforts demonstrating efficiencies exceeding 30% for solar-hydrogen generation³⁻⁷ and 23% for carbon-based solar fuels.⁸⁻¹¹ Despite these advancements in peak efficiency, substantial technological leaps must still be made in the domain of device longevity, as stabilizing the operation of photoelectrochemical (PEC) devices will be critical for realizing economically competitive solar fuel production.^{12,13} Devices with lifetimes on the order of 10 to 30 years have been estimated in various techno-economic assessments as essential requirements for the utility-scale implementation of PEC technologies.¹⁴⁻¹⁶ However, device degradation and activity losses are commonly determined by monitoring the device current, a quantity masking the relative contributions of photovoltaic (PV)

deactivation and electrocatalyst activity drops to overall performance losses. For example, in a conventional, liquid-fed PEC system, gas bubbles may obscure the PV while blocking catalytic areas at the same time. In this study, an approach granting insight into the various causes for PEC device efficiency losses is described. In particular, the causes for observed fluctuations in device performance are determined through the collection of real-time polarization data paired with an analytical method that permits the quantitative decomposition of drops in device current into its constituent PV- and catalyst-driven performance losses. We test the validity of this approach by applying it to data collected for an integrated, photoelectrochemical device for hydrogen evolution, operating under conditions of simulated, 1-sun illumination.¹⁷

Briefly, the device used for testing this loss analysis procedure consisted of a multi-junction photovoltaic integrated into a proton exchange membrane, with catalyst-coated carbon papers being compressed against both sides of the membrane, as previously reported by the authors.¹⁷ The datasets used for this study were derived from

a device configuration in which electrocatalysis was facilitated by a water vapor feed instead of liquid water, which we have found to significantly increase the device stability. Specifically, a humidified gas feed was realized by bubbling nitrogen carrier gas through a heated ($\sim 70^\circ\text{C}$) glass vial before it reached the anode. In this particular device, illumination proceeds from the cathode side. Illumination by the solar simulator results in a device surface temperature that stabilizes at approximately 40°C , resulting in the partial condensation of water vapor in the anode due to the temperature difference between the device and the humidified gas feed.

During unbiased operation of this PV-integrated membrane (PIM) device, two reversible loss mechanisms were influenced by the humidification of the system. Low humidification levels forced the dehydration of the Nafion membrane, with a resultant decrease in membrane ionic conductivity, as water gets removed from the hydrophilic, negatively charged channels that enable the selective transfer of cations.^{18,19} These increased impedances to ion flow correspond to higher overpotentials for electrochemical oxygen and hydrogen evolution reactions at the respective anode and cathode surfaces. The ultimate result is an operating point that occurs at lower current densities, decreasing the overall device efficiency. Low relative humidity conditions in the cell may also reduce the amount of useable catalyst surface area, compounding reductions in the device performance.²⁰ A previous report suggests that feed conditions above 80% relative humidity are required to reach desirable current densities in vapor-fed PEC devices.²¹ Here, the device was operated slightly above the condensation threshold to ensure sufficient hydration of the system, even when the cathode chamber was purged by dry nitrogen gas. Under these conditions, water transport through the membrane increased considerably due to the relative humidity gradient and the proton-induced, electro-osmotic drag of water across the membrane.²² As a result of water transport through the membrane, a similar amount of water was observed in the vapor traps located between the cathode and anode outlets and the gas chromatograph. Consequently, if the temperature of the bubble humidifier is set too high, water can condense on the PV front at the cathode side, partially blocking the incident light and reducing the device efficiency. Optimizing device performance requires a complete understanding of loss mechanisms, highlighting the importance of deconvoluting the contributions of electrochemical and PV-driven performance losses to the observed drops in the overall device current.^{23,24} For this reason, the operating voltage and current were logged concurrently throughout a 180-h experiment. The resulting current–voltage readouts for the first 100 h of operation are plotted along with the initial electrochemical (EC) and photovoltaic (PV) polarization curves in Fig. 1, while the remaining 80 h are displayed in Fig. S1. In order to maintain visibility, the values for the operating point were averaged every 12 min, resulting in a total of 500 plotted points. Generally, a higher operating voltage indicates conditions that are too dry, with the overpotential for the electrochemical reactions increasing, resulting in EC-based current losses. However, when feed conditions are too humid, condensation of water vapor attenuates the incident light, forcing corresponding reductions in PV performance, as evidenced through current drops at relatively low operating voltages.

The modeled PV curves at various levels of water condensation shown in Fig. 1, resulting in certain degrees of light

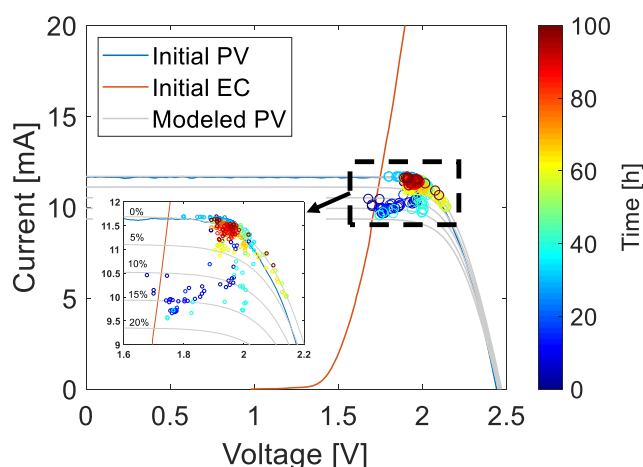


FIG. 1. Operating point during the first 100 h of unbiased operation compared to the electrochemical (EC) and photovoltaic (PV) polarization curves taken before operation and modeled PV curves at different levels of water vapor condensation at the PV front. The deviation at higher voltages between the dry, initial PV curve and the modeled, 0% attenuation curve is due to the higher (30 mV) open circuit voltage (V_{oc}) of the PV upon humidification. The PV is cooled by $\sim 4^\circ\text{C}$ during operation, compared to the dry conditions, resulting in the higher V_{oc} .

attenuation (shading), are calculated based on the characteristic PV parameters, determined prior to the operation of the PEC device. For the determination of the characteristic PV parameters such as series resistance (R_s), shunt resistance (R_{sh}), and ideality factor (n), I–V curves were taken at different levels of water condensation at the PV illumination side (Fig. S2). The PV parameters for each of these different light attenuation cases were then extracted from the PV's I–V curves by conducting a least-squares fit of the experimental data to the single-diode solar cell model^{25–27} using a custom MATLAB script. The resulting values for these three parameters in each of the light attenuation cases examined remain essentially constant, with light attenuation mainly affecting the observed short circuit current. Therefore, changes in the PV polarization response at different humidification levels were not a result of fluctuating values of R_s , R_{sh} , or n , allowing for the general modeling of PV polarization curves at different levels of unspecified PV illumination. The characteristic values for R_s , R_{sh} , and n taken at various humidity levels were averaged and are presented in Table S1.

In Fig. 2(a), PV curves with varying levels of light attenuation are plotted together with one operating point, which is found to lie on the 15% light attenuation curve and shows both EC and PV losses. The difference in current between the operating point and a point at the same voltage, but on the unshaded, 0% PV curve, may be seen as the current lost due to PV shading. In contrast, the EC losses are calculated by comparing the operating point with a point on the same light attenuation curve, but at the required minimum voltage of 1.229 V to split water, and subtracting the respective currents. The PV parameters were then used to reconstruct the best-fitting PV I–V curve for each current–voltage data pair during operation. In Fig. 2(b), the calculated PV and EC losses for each operating point are plotted between the short circuit current (I_{sc}) of the PV, which

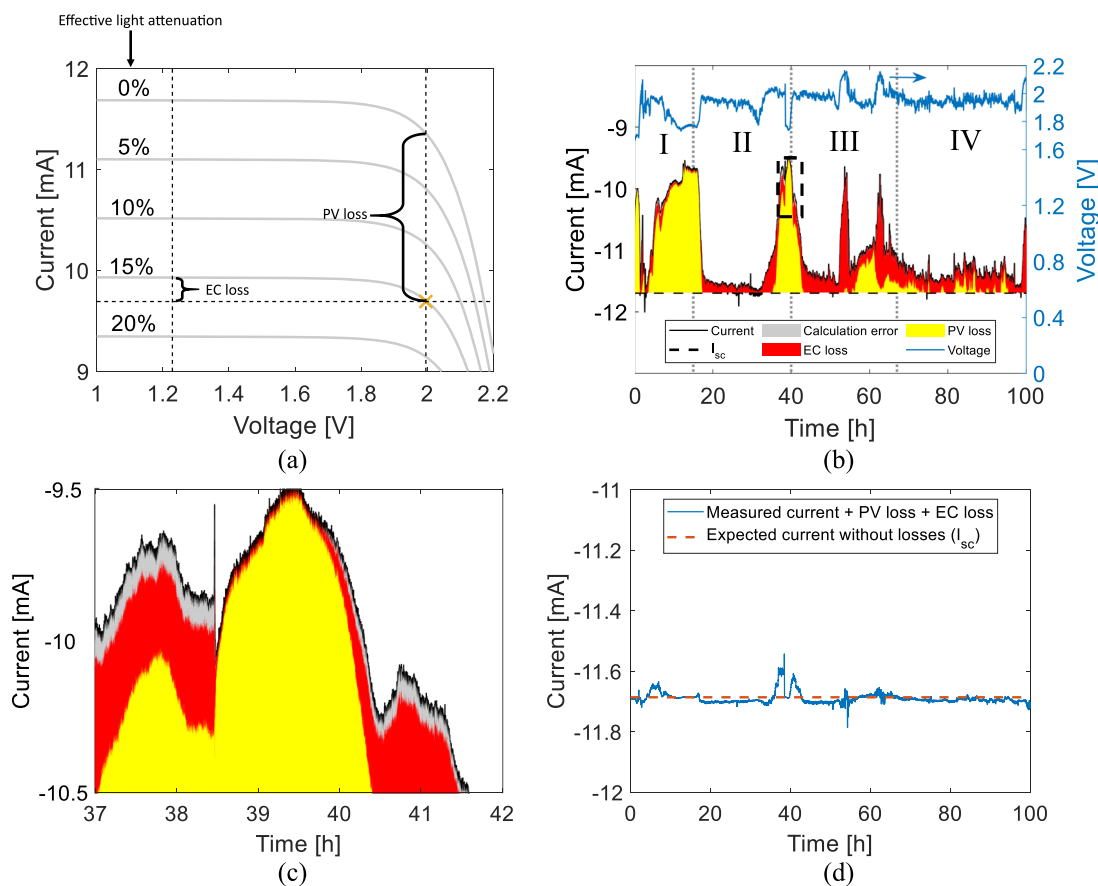


FIG. 2. Deconvolution of current losses through concurrent logging of voltage and current during device operation. (a) Loss calculation example for one operating point, dividing the total current loss into PV and EC losses. (b) Calculated current losses during the first 100 h of operation, filling the area between the short circuit current (I_{sc}) of the PV and the operating current. Roman numbers indicate the different temperatures of the bubble humidifier (I: 75 °C, II: 70 °C, III: 65 °C, and IV: 70 °C). (c) Magnification of the highlighted area in Fig. 2(b) indicating the minimal calculation error. (d) Calculation error during the first 100 h of operation shown by the difference between I_{sc} of the PV and the measured current plus accounted losses.

marks the maximum achievable PEC current, and the measured net current during operation. As expected, PV losses dominate at relatively low operating voltages, while EC losses increase significantly at operating voltages exceeding 2 V. After the first 15 h of the experiment, during which the condensation of water vapor reduced the intensity of light reaching the PV, the temperature of the bubble humidifier was decreased from 75 °C to 70 °C. A lower temperature resulted in reduced water content of the anode feed, followed by less condensation at the cathode side of the PEC cell. After 40 h, the temperature was decreased to 65 °C, as increasing condensation again caused elevated PV losses. However, the reduced water content of the nitrogen carrier at this temperature is found to cause membrane dehydration, promoting EC losses after 50 h. Therefore, the temperature was readjusted to 70 °C after 67 h, resulting in low overall losses for the following 30 h. As shown in Figs. 2(b) and 2(c), device losses that go unaccounted for using our approach are found to be negligible and are likely artifacts of minor calculation errors, arising from the least-squares fitting process that is central to our loss deconvolution methodology. In Fig. 2(d), the short circuit current is

compared against the measured current plus the current associated with PV and EC losses. The difference between the two lines equals the calculation error and is below 0.1 mA during the entire 100 h. Similarly, the calculation error accounts for only 1% of the integral between the operating current and I_{sc} , signifying that about 99% of all current losses were captured. In addition, this loss deconvolution method was successfully applied to a second, liquid-fed device architecture (Fig. S3),²⁸ and a control experiment was conducted (Fig. S4).

Due to the concurrent logging of operating voltage and current, the partitioning of time-dependent efficiency drops into PV and electrochemical losses was possible, using a new loss deconvolution methodology. Feed humidification conditions were found to have a great effect on both loss mechanisms. PV attenuation losses were caused by the condensation of water vapor at the PV illumination side, while EC losses are a result of Nafion membrane dehydration, rather than losses in catalyst activity. It must be noted that intrinsic stability of the photoabsorber is a key assumption of this analytical approach, as it treats the extracted parameters found through

fitting an experimental PV load curve to the Shockley-diode equation as time-independent constants, with PV performance drops only being influenced by changes in the effective incident light intensity. This particular case may not apply to chemically/temporally unstable photoabsorbers, where it may reasonably be expected that attributes such as the shunt resistance, ideality factor, and series resistance change over the course of PV degradation. In such cases, it would be necessary to periodically re-measure the PV polarization response and extract the altered diode parameters, before this methodology could be meaningfully applied. Similarly, if the incident light intensity is not constant, such as during outdoor, diurnal experiments, it needs to be determined constantly, for example, with a calibrated reference cell, to separate PV losses from lower irradiation conditions.

This newly established capability, which captures the time-dependence of the loss mechanisms in play during PEC device operation, opens the door for real-time adjustments to the feed humidity that appropriately compensate for the type of loss driving performance degradation. Such efforts will be the focus of future investigations. Finally, this loss separation technique should be applicable to a range of solar-driven devices, provided that current–voltage data are collected during operation. Aside from the monolithic PEC device explored in this study, this approach should also be relevant to wired integrated PEC devices and PV-coupled electrolyzer units.

See the [supplementary material](#) for the determination of characteristic PV parameters and demonstration of the loss analysis methodology with a second device architecture.

The authors thank Jason Cooper and Ian Sharp for their helpful insights. The authors gratefully acknowledge research support from the Joint Center for Artificial Photosynthesis (JCAP), a DOE Energy Innovation Hub, supported through the Office of Science of the U.S. Department of Energy under Award No. DE-SC0004993.

DATA AVAILABILITY

The data that support the findings of this study are available from the corresponding author upon reasonable request.

REFERENCES

- ¹A. Fujishima and K. Honda, *Nature* **238**, 37 (1972).
- ²A. Fujishima and K. Honda, *Bull. Chem. Soc. Jpn.* **44**, 1148 (1971).
- ³J. Jia, L. C. Seitz, J. D. Benck, Y. Huo, Y. Chen, J. W. D. Ng, T. Bilir, J. S. Harris, and T. F. Jaramillo, *Nat. Commun.* **7**, 13237 (2016).
- ⁴O. Khaselev and J. A. Turner, *Science* **280**, 425 (1998).
- ⁵S. Licht, B. Wang, S. Mukerji, T. Soga, M. Umeno, and H. Tributsch, *J. Phys. Chem. B* **104**, 8920 (2000).
- ⁶J. L. Young, M. A. Steiner, H. Döscher, R. M. France, J. A. Turner, and T. G. Deutsch, *Nat. Energy* **2**, 453 (2017).
- ⁷W.-H. Cheng, M. H. Richter, M. M. May, J. Ohlmann, D. Lackner, F. Dimroth, T. Hannappel, H. A. Atwater, and H.-J. Lewerenz, *ACS Energy Lett.* **3**, 1795 (2018).
- ⁸M. Asadi, M. H. Motevaselian, A. Moradzadeh, L. Majidi, M. Esmaeilirad, T. V. Sun, C. Liu, R. Bose, P. Abbasi, P. Zapol, A. P. Khodadoust, L. A. Curtiss, N. R. Aluru, and A. Salehi-Khojin, *Adv. Energy Mater.* **9**, 1803536 (2019).
- ⁹G. Gurudayal, J. W. Beeman, J. Bullock, H. Wang, J. Eichhorn, C. Towle, A. Javey, F. M. Toma, N. Mathews, and J. W. Ager, *Energy Environ. Sci.* **12**, 1068 (2019).
- ¹⁰M. Schreier, F. Héroguel, L. Steier, S. Ahmad, J. S. Luterbacher, M. T. Mayer, J. Luo, and M. Grätzel, *Nat. Energy* **2**, 855 (2017).
- ¹¹Y. Wang, J. Liu, Y. Wang, Y. Wang, and G. Zheng, *Nat. Commun.* **9**, 5003 (2018).
- ¹²Y.-H. Chiu, T.-H. Lai, M.-Y. Kuo, P.-Y. Hsieh, and Y.-J. Hsu, *APL Mater.* **7**, 080901 (2019).
- ¹³F. Nandjou and S. Haussener, *J. Phys. D: Appl. Phys.* **50**, 124002 (2017).
- ¹⁴B. A. Pinaud, J. D. Benck, L. C. Seitz, A. J. Forman, Z. Chen, T. G. Deutsch, B. D. James, K. N. Baum, G. N. Baum, S. Ardo, H. Wang, E. Miller, and T. F. Jaramillo, *Energy Environ. Sci.* **6**, 1983 (2013).
- ¹⁵B. D. James, G. N. Baum, J. Perez, and K. N. Baum, *Technoeconomic Analysis of Photoelectrochemical (PEC) Hydrogen Production* (Directed Technologies, Inc., 2009).
- ¹⁶M. R. Shaner, H. A. Atwater, N. S. Lewis, and E. W. McFarland, *Energy Environ. Sci.* **9**, 2354 (2016).
- ¹⁷T. A. Kistler, N. Danilovic, and P. Agbo, *J. Electrochem. Soc.* **166**, H656 (2019).
- ¹⁸C. Heitner-Wirguin, *J. Membr. Sci.* **120**, 1 (1996).
- ¹⁹J. Larminie and A. Dicks, *Fuel Cell Systems Explained*, 2nd ed. (Wiley, Chichester, 2003).
- ²⁰G. Heremans, C. Trompoukis, N. Daems, T. Bosserez, I. F. J. Vankelecom, J. A. Martens, and J. Rongé, *Sustainable Energy Fuels* **1**, 2061 (2017).
- ²¹J. M. Spurgeon and N. S. Lewis, *Energy Environ. Sci.* **4**, 2993 (2011).
- ²²Z. Qi, *Proton Exchange Membrane Fuel Cells*, 1st ed. (CRC Press, Boca Raton, FL, 2014).
- ²³Z. Wang, M. Lyu, P. Chen, S. Wang, and L. Wang, *Phys. Chem. Chem. Phys.* **20**, 22629 (2018).
- ²⁴W. Cui, W. Niu, R. Wick-Joliat, T. Moehl, and S. D. Tilley, *Chem. Sci.* **9**, 6062 (2018).
- ²⁵F. F. Muhammad, A. W. Karim Sangawi, S. Hashim, S. K. Ghoshal, I. K. Abdullah, and S. S. Hameed, *PLoS One* **14**, e0216201 (2019).
- ²⁶A. Ben Or and J. Appelbaum, *Prog. Photovoltaics* **21**, 713 (2013).
- ²⁷M. T. Winkler, C. R. Cox, D. G. Nocera, and T. Buonassisi, *Int. J. Hydrogen Energy* **110**, E1076–E1082 (2013).
- ²⁸T. A. Kistler, D. Larson, K. Walczak, P. Agbo, I. D. Sharp, A. Z. Weber, and N. Danilovic, *J. Electrochem. Soc.* **166**, H3020 (2019).